Applicability of analytical protocols for the characterisation of carbon-supported platinum group metal fuel cell electrocatalysts

M. Williams[a*], L. Khotseng[a], Q. Naidoo[b], L. Petrik[b], A. Nechaev[b,c] and V. Linkov[a]

The nanoparticulate size of fuel cell electrocatalysts raises significant challenges in the analytical techniques used in their structural and electrochemical characterisation. For this reason, the applicability of analytical protocols in the qualitative and quantitative characterisation of nanophase fuel cell electrocatalysts was investigated. A set of structural and chemical properties influencing the performance of the electrocatalysts was identified. A large range of analytical tools was employed in characterising the electrocatalysts of interest. High accuracy and precision in the quantitative and qualitative structural and electrochemical characterisation of Pt/C and Pt-Ru/C nanophase electrocatalysts was demonstrated. Certain techniques were deemed to be highly applicable in discriminating between high- and low-performance electrocatalysts based on their structural and electrochemical properties. The goal of this effort is to contribute to the development of South Africa's capabilities in the emerging hydrogen economy.

Key words: nanophase, electrocatalyst, platinum group metals, characterisation

Introduction

At the forefront of renewable energy strategies is the hydrogen economy, including polymer electrolyte membrane fuel cell (PEMFC) technology, which offers an attractive form of energy generation and could satisfy the growing energy demand without the emission of harmful byproducts. For South Africa to participate as a partner in the envisaged world hydrogen economy and in critical development of the PEMFC, diversification of local platinum group metal (PGM) resources for employment in PEMFC electrocatalysis is of the utmost importance. The goal of this effort is to contribute to the development of South Africa's capabilities in this emerging economy and to motivate commercial and financial investment into South Africa.

To enhance physicochemical properties and reduce operational costs, PGM electrocatalyst particle sizes are decreased to the nanometre domain, thereby increasing the overall active surface area. With the introduction of the electrocatalyst particle size into the nanometre domain, the characterisation of the altered structural and electrocatalytic properties gains significant importance. This significance stems from the fact that most engineered 'nanomaterials' have a functionality based on their structural physicochemistry. Progress from fabrication to commercialisation is often derailed by the difficulties associated with characterising nanophase electrocatalysts. This is due to size hampering the use of many well-established analytical techniques. The characterisation of nanophase electrocatalysts raises significant challenges in identifying the analytical tools and fundamental methods used in their investigation. It is therefore necessary to establish an analytical protocol by which the physicochemical properties of fabricated nanophase electrocatalysts could be characterised. In doing so, the standardised characterisation protocol will facilitate the collection of comparable results.

Ideally, a minimum set of properties is considered essential because it is impractical, albeit laudable, to characterise every property of nanophase electrocatalysts. Physicochemical properties which may influence nanophase electrocatalyst behaviour include particle size, surface composition, surface area, surface dispersion, electrocatalytic activity,[1] porosity,[2] state of agglomeration, crystal structure, catalytic activity and surface chemistry.[3]

In this study the minimum set of physicochemical properties of nanophase electrocatalysts, governing the observed physicochemical behaviour, were characterised. It is with this in mind that the applicability of analytical tools for the qualitative and quantitative characterisation of current and prospective nanophase electrocatalysts was investigated.

Methods

The investigation was initiated by the structural and electrochemical characterisation of carbon-supported platinum (Pt/C), platinum-ruthenium (Pt-Ru/C) and carbon nanotube-supported platinum (Pt/CNT) nanophase fuel cell electrocatalysts.

Commercially-available carbon-supported platinum (JM Pt_{40}/C) and platinum-ruthenium (JM $Pt_{30}Ru_{15}$/C) electrocatalysts (Johnson Matthey™, Fuel Cell Grade) served as standardised model materials of known properties. Their use in the study allowed for the evaluation of the applicability of various analytical techniques for the characterisation of nanophase electrocatalysts. In addition, their properties served as benchmarks against which that of all fabricated materials could be compared.

Carbon-supported nanophase Pt electrocatalysts (Pt/C) were prepared through an impregnation-reduction technique by suspending treated carbon black (Cabot Vulcan® XC-72) in a solvent (glycol/*iso*-propanol), a metal precursor ($H_2PtCl_6{\cdot}6H_2O$) and a pH-regulator (H_2SO_4 or NaOH). Formaldehyde reduction ensured the deposition of Pt onto the carbon black support material.[4,5]

Carbon-supported nanophase Pt-Ru/C electrocatalysts were prepared using an impregnation-reduction technique in which $H_2PtCl_6{\cdot}6H_2O$, $RuCl_3{\cdot}3H_2O$, 25% (v/v) *iso*-propanol/H_2O, and treated carbon black were mixed into a slurry and Pt-Ru nanoparticles were reduced onto the carbon support using formaldehyde at 80°C for 30 min.[6]

CNT-supported Pt electrocatalysts were prepared using an impregnation-reduction technique.[4,5] The multi-walled CNT support materials were prepared by nebulised spray pyrolysis of a ferrocene-toluene (20.00 g l^{-1}) solution at 900°C in a quartz tube reactor. Argon was used as the carrier gas. The nebuliser frequency was 1.6 MHz and the total reaction time was 45 min.[7] The treated CNT was then suspended in 1-propanol, $H_2PtCl_6{\cdot}6H_2O$ and H_2SO_4. Platinum was deposited onto CNT by formaldehyde reduction. CNT-supported nanophase Pt

[a]South African Institute for Advanced Materials Chemistry, Faculty of Science, University of the Western Cape, Private Bag X17, Bellville 7535, South Africa.
[b]Environmental and Nano Sciences Group, Department of Chemistry, Faculty of Science, University of the Western Cape, Private Bag X17, Bellville 7535, South Africa.
[c]Materials Research Group, iThemba LABS, P.O. Box 722, Somerset West 7129, South Africa.
*Author for correspondence E-mail: 2438658@uwc.ac.za

electrocatalysts were compared to Pt-plated CNT electrocatalysts, prepared using an electroless-plating technique.[8]

A range of analytical techniques were utilised in the characterisation of nanophase electrocatalysts. Crystal structure and metal particle size were investigated using X-ray diffraction (XRD). Topography and surface microstructure were studied using scanning electron microscopy (SEM). Metal particle size, particle size distribution and metal dispersion were investigated using transmission electron microscopy (TEM), and total surface area and porosity by N_2-physisorption. Topography and surface elemental distribution of electrocatalyst cast-films were studied using particle-induced X-ray emission spectroscopy (micro-PIXE). Topography and surface activity of electrocatalyst cast-films were evaluated using scanning electrochemical microscopy (SECM). Surface chemical state was studied using temperature-programmed reduction (TPR). Electrocatalytic activity was evaluated using cyclic voltammetry (CV).

Results and discussion

Crystallinity can be directly studied using diffraction techniques such as XRD. Quantitative information extracted using XRD was of high accuracy and precision and gave valuable insight into the crystallographic properties of the electrocatalysts and influence of alloying on the crystallographic structure. The corresponding diffractograms are presented in Fig. 1. For JM $Pt_{30}Ru_{15}$/C, the diffraction peaks corresponding to the characteristic hexagonal-closest-packing structure of Ru were absent, confirming the complete alloying of Ru into the face-centered cubic lattice of Pt.[9,10] Peak shifts were observed in JM $Pt_{30}Ru_{15}$/C, compared to JM Pt_{40}/C, and were indicative of high degrees of alloying, similar to that observed by Tsou *et al.* [11] and Guo *et al.*[12] The particle size was calculated as 4.2 nm and 3.5 nm for JM Pt_{40}/C and JM $Pt_{30}Ru_{15}$/C, respectively, as compared to the manufacturers' specifications of 4.5 nm and 4.0 nm.[13] X-ray diffraction was therefore able to perform accurate analyses in the nanometre domain and forms an integral part in a comprehensive characterisation of nanophase electrocatalysts.

Metal particle size and distribution play important roles in catalytic efficiency due to the relationship between catalytic activity and surface structure. These properties are best studied using fundamental characterisation tools such as electron microscopy. Transmission electron microscopy exhibited both high precision and accuracy in the determination of particle size. Values were reproducible and agreed well with those determined by others.[12–14] Also, there was good agreement between particle sizes determined using XRD and TEM.

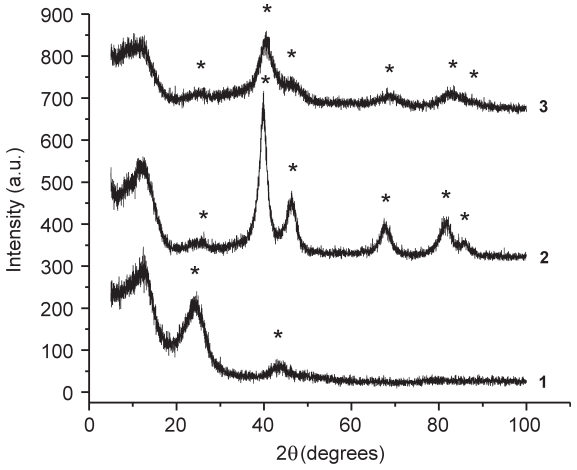

Fig. 1. Diffractograms of Pt-based fuel cell electrocatalysts: (1) Vulcan® XC-72, (2) JM Pt_{40}/C and (3) JM $Pt_{30}Ru_{15}$/C (λ = 1.1518 Å, scan rate = 0.05 degrees min^{-1}). Peaks are indicated by *.

Metal nanoparticles, in JM Pt_{40}/C and JM $Pt_{30}Ru_{15}$/C, were found to be well dispersed on the carbon support (Fig. 2). Large agglomerates were also observed in certain areas of the samples. Nanoparticles generally ranged between 2–7 nm in size, with average particle sizes of 4.2 nm and 4.0 nm for JM Pt_{40}/C and JM $Pt_{30}Ru_{15}$/C, respectively. Metal surface areas of 64–70 $m^2\ g^{-1}$ were determined.[15] In comparison, the average JM Pt_{40}/C metal particle size specified by the supplier, Johnson Matthey, was 4.5 nm with a metal surface area of 62 $m^2\ g^{-1}$.[13] Experimental values were thus of good accuracy.

Metal nanoparticles were also observable using ultrahigh-vacuum, high-resolution SEM. An average Pt particle size of 6.2 nm was observed when depositing Pt nanoparticles, using formaldehyde reduction of $H_2PtCl_6{\cdot}6H_2O$, on carbon nanotube support materials, denoted Pt/CNT in this study (Fig. 3). Also observable were large Pt agglomerates on the surface of the CNT support material. The agglomeration was a result of the thermodynamic instability of metal nanoparticles. Unfortunately, the agglomeration is unavoidable and occurs spontaneously in the preparation process. The observations described illustrated the applicability of high-resolution SEM in the direct determination of metal particle size and distribution on carbon-supported fuel cell electrocatalysts.

Surface area and porosity, in combination with electrochemical information, can be used to illustrate a relationship between surface microstructure and catalytic activity of supported nanophase electrocatalysts. N_2 physisorption was found to

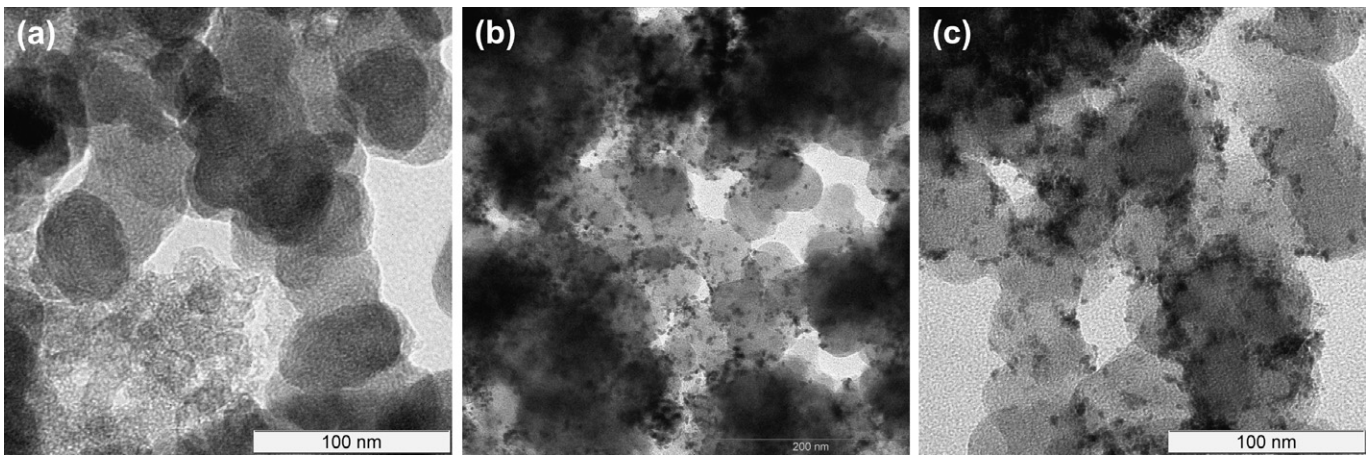

Fig. 2. Transmission electron microscopy images of: (**a**) Vulcan® XC-72, (**b**) JM Pt/C and (**c**) JM Pt-Ru/C nanophase electrocatalysts (200 kV, 20 μA).

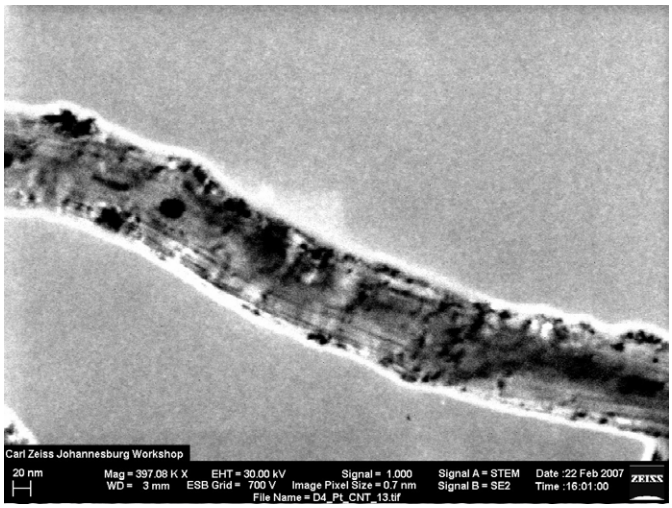

Fig. 3. High-resolution SEM image of Pt/CNT nanophase electrocatalyst (30 kV, 30 mm).

produce highly-accurate surface area and pore size distribution data. According to Jordan *et al.*[16] and Cabot™ Corporation, Vulcan XC-72® support material with particle sizes ∅ = 30–75 nm corresponded to a surface area of 250–300 $m^2\ g^{-1}$. In contrast, the measured Brunauer-Emmer-Teller (BET) surface area of Vulcan XC-72® was 242 $m^2\ g^{-1}$, corresponding to particle sizes of 50–60 nm, determined via TEM. Measured BET surface areas corresponded well with those obtained by Li *et al.*,[4] Prabhuram *et al.*[15] and Jordan *et al.*,[16] which were 237 $m^2\ g^{-1}$, 250 $m^2\ g^{-1}$ and 250–300 $m^2\ g^{-1}$, respectively. In comparison, JM Pt_{40}/C and JM $Pt_{30}Ru_{15}$/C exhibited relatively small surface areas (132 $m^2\ g^{-1}$ and 106 $m^2\ g^{-1}$) compared to Vulcan® XC-72. Lowered internal pore areas were observed in JM Pt_{40}/C and JM $Pt_{30}Ru_{15}$/C with average pore sizes of 15.6 nm and 17.3 nm, respectively. The mesoporous structure of the fuel cell electrocatalysts was confirmed.[13]

Micro-PIXE was used in the investigation of the surface topography and elemental distribution of electrocatalyst cast-films prepared by suspending the nanophase electrocatalysts in alcoholic Nafion® solution (Fig. 4). The surface of the JM Pt_{40}/C cast-film was observed as being fairly homogeneous in terms of elemental distribution, without significant agglomeration. Cracks of about 2 μm in width were observed in the JM Pt_{40}/C cast-film and were due to differences in the coefficients of expansion between the cast film and highly-oriented pyrolytic

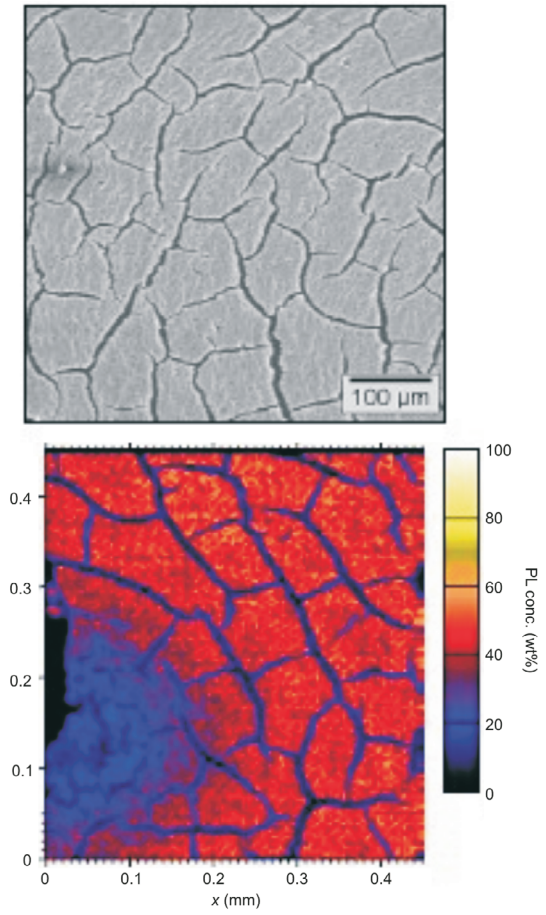

Fig. 4. (**a**) Scanning electron microscopy image of a JM Pt_{40}/C electrocatalyst cast film and (**b**) micro-PIXE surface elemental distribution map of a JM Pt_{40}/C electrocatalyst cast film (3.0 MeV).

graphite current collector after removal of the solvent. Particle-induced X-ray emission spectroscopy allowed for the discrimination of elemental dispersion across the surface of electrocatalyst cast films. This type of information may help in the understanding of the chemical behaviour at the interface between the proton-conducting membrane and the catalyst layers of the PEMFC.

Scanning electrochemical microscopy was used to qualitatively characterise cast films, prepared from nanophase electrocatalysts, in terms of topography and surface activity. The

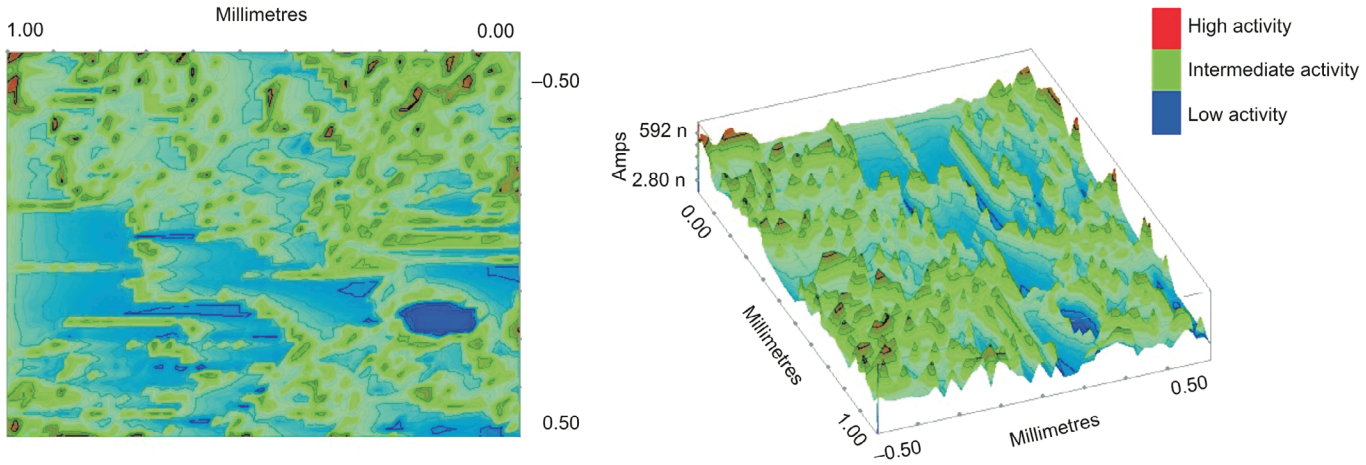

Fig. 5. Scanning electrochemical microscopy map of JM Pt_{40}/C cast film on highly oriented pyrolytic graphite (HOPG) (E_{UME} = –0.65 $V_{Ag/AgCl}$; E_{HOPG} – 0.0 $V_{Ag/AgCl}$, raster speed = 5.0 µm s^{-1}, tip-substrate separation = 5.0 µm).

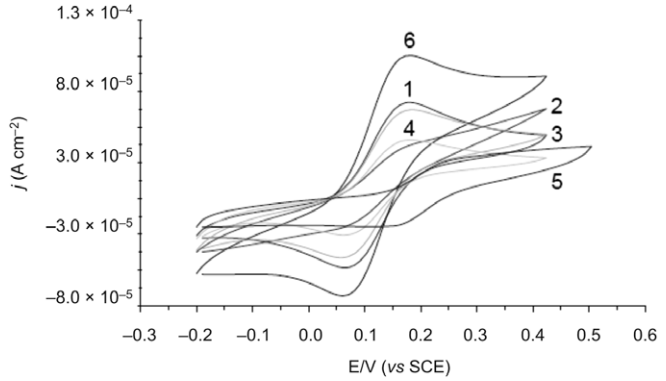

Fig. 6. Voltammograms for electrochemical evaluation of supported Pt nanophase electrocatalysts in 0.01M $K_4[Fe(CN)_6]$ supported in 0.1M KCl (sweep rate = 20 mV s^{-1}): (1) JM Pt/C, (2) Pt/C (glycol), (3) Pt/C (1-PrOH, H_2SO_4, pH 2), (4) Pt/C (1-PrOH, NaOH, pH 12), (5) Pt-plated CNT and (6) Pt/CNT.

topography of the JM Pt_{40}/C electrocatalyst cast film prepared was studied using the imaging mode in SECM. Ultra-microelectrodes were fabricated by sealing 10-mm lengths of Pt micro-wire ($\varnothing = 25\,\mu$m) in evacuated borosilicate glass capillary tubes and polishing using diamond emery paper and alumina pastes to produce a fine truncated tip with an exposed Pt disk. The SECM map for the study of the topography of a cast film prepared using JM Pt_{40}/C is presented in Fig. 5. The JM Pt_{40}/C cast film exhibited areas of high activity, due to agglomeration, which produced maximum perturbation in the ultramicroelectrode (UME) tip current. A range of electrochemical activities was observed over the SECM map, indicative of a heterogeneous surface.

It was very difficult to extract quantitative chemical information from the SECM data. For this reason SECM was relegated to a qualitative role in the characterisation of nanophase electrocatalysts. However, SECM is also a useful technique to determine the degree and quality of dispersion of the supported electrocatalyst in a cast film over small surface areas.

Chemisorptive characterisation of supported nanophase electrocatalysts was conducted using TPR. Temperature-programmed reduction analysis of JM Pt_{40}/C and JM $Pt_{30}Ru_{15}$/C was undertaken to ascertain the number of oxidation states on the catalyst surface. Two events were detectable in the TPR profile of JM Pt_{40}/C: $Pt^{4+} \rightarrow Pt^{2+}$ transition at low temperature, and $Pt^{2+} \rightarrow Pt^{0}$ transition at high temperature. In the TPR profile of JM $Pt_{30}Ru_{15}$/C four peaks were observed: $Pt^{4+} \rightarrow Pt^{2+}$ and $Pt^{2+} \rightarrow Pt^{0}$ transitions at high temperature, and $Ru^{3+} \rightarrow Ru^{0}$ and $Ru^{4+} \rightarrow Ru^{0}$ transitions at low temperature[17]. Temperature-programmed reduction was successfully employed in the speciation of nanophase fuel cell electrocatalysts.

Cyclic voltammetry was used to probe surface reactions under well-controlled conditions, giving insight into the catalytic activity of nanophase fuel cell electrocatalysts.[18,19] The CV analysis was conducted in 0.01M $K_4[Fe(CN)_6]$, diluted in 0.1M KCl supporting electrolyte, to assess the quality of fabricated nanophase electrocatalysts. The applied potential was generally swept between –0.20 V_{SCE} and 0.6 V_{SCE} at a sweep rate of 20 mV s^{-1}. The working electrode was glassy carbon, the reference electrode was saturated calomel and the counter electrode was a Pt-wire basket. Results obtained from different electrocatalysts were collected in replicate and the most reproducible value presented in each case. Results were presented and tabulated in Fig. 6 and Table 1, respectively.

To summarise, Pt/CNT and Pt/C (1-PrOH/H_2SO_4/pH2) exhibited

Table 1. Summary of the electrochemical data collected in the electrochemical evaluation of supported Pt nanophase electrocatalysts in 0.01M $K_4[Fe(CN)_6]$ supported in 0.1M KCl (j_{PA} = current density; ΔE_P = peak separation; E^0 = formal potential)

Electrocatalyst	j_{PA} (μA cm^{-2})	j_{PA}/j_{PC}	E_{PA} (V)	ΔE_P (V)	E^0 (V)
JM Pt_{40}/C	67.2	1.38	0.180	0.118	0.121
Pt/C (glycol)	37.6	1.87	0.183	0.120	0.123
Pt/C(1-PrOH/NaOH/pH12)	40.9	1.60	0.180	0.117	0.122
Pt/C(1-PrOH/H_2SO_4/pH2)	62.2	1.50	0.184	0.124	0.122
Pt/CNT	100	1.46	0.179	0.117	0.121
Pt-plated CNT	34.1	1.82	0.247	0.085	0.205

catalytic activities greater or comparable to that of JM Pt_{40}/C. Carbon-supported Pt nanophase electrocatalysts prepared using 1-propanol as a solvent exhibited slightly higher activities than those prepared using glycol as a solvent. Importantly, catalytic activity was affected by the pH used in the preparation step, and electrocatalysts prepared from acidic solution exhibited markedly higher catalytic activity compared to electrocatalysts prepared from alkaline solution. This is due to differences in surface functional groups. The impregnation-reduction method produced superior CNT-supported catalysts compared to those produced by electroless-plating. And finally, the fabricated Pt-Ru/C was inferior to the JM $Pt_{30}Ru_{15}$/C and the preparation method therefore required further investigation.

Results illustrated that CV analysis was able to quantitatively discriminate between the activities of various fabricated nanophase fuel cell electrocatalysts and can be applied as a tool to optimise catalyst preparation. Also, preparation variables could be critically evaluated and optimised for future fabrication of cost-effective highly-active nanophase fuel cell electrocatalysts.

Conclusions

In conclusion, the applicability of the identified analytical techniques in the characterisation of nanophase fuel cell electrocatalysts was investigated. Techniques such as XRD, TEM, SEM, TPR, SECM, micro-PIXE, N_2-physisorption, and CV were used in this study and were confirmed to be highly applicable in the qualitative and quantitative characterisation of the nanophase sample materials. These techniques were also effective in discriminating between high- and low-activity electrocatalysts, based on the structural-chemical relationship of nanomaterials. A detailed strategy, or protocol, for the characterisation of nanophase electrocatalysts was successfully designed. It is recommended that this strategy and the experimental methodologies used in this study be implemented in future characterisation studies of fabricated nanophase fuel cell electrocatalysts. This study also showed that a capacity to prepare nanophase fuel cell electrocatalysts and accurately characterise them has been developed in South Africa.

We thank the National Research Foundation, South Africa and ESKOM for funding and iThemba LABS, Veeco Zeiss, and the Chemistry and Physics Departments at the University of the Western Cape for characterisation support.

Received 18 May. Accepted 26 May 2009.

1. The Center for Nanotechnology at the University of Washington (2005). Fabrication and characterisation of nanomaterials. Washington. Online at: https://www.engr.washington.edu/epp/nano/jan_04.html.
2. Oberdöster G., Maynard A. and Donaldson K. (2005). Principles for characterizing the potential human health effects from exposure to nanomaterials: elements of a screening strategy. *Part. Fibre Toxicol.* **2**, 8.
3. Haber J. (1991). Manual on catalyst characterization. *Pure Appl. Chem.* **63**, 1227–1246.
4. Li W., Zhou W., Li H., Zhou Z., Zhou B., Sun G. and Xin Q. (2004). Nano-

structured Pt-Fe/C as cathode catalyst in direct methanol fuel cell. *Electrochim. Acta* **49**, 1045–1055.

5. Zhou W.J., Zhou B., Li W.Z., Zhou Z.H., Song S.Q., Sun G.Q., Xin Q., Douvartzides S., Goula M. and Tsiakaras P. (2004). Performance comparison of low-temperature direct alcohol fuel cells with different anode catalysts. *J. Power Sources* **126**, 16–22.
6. Guo J., Sun G., Wang Q., Wang G., Zhou Z., Tang S., Jiang L., Zhou B. and Xin Q. (2006). Carbon nanofibers supported Pt–Ru electrocatalysts for direct methanol fuel cells. *Carbon* **44**, 152–157. Online at: http://www.sciencedirect.com/science/journal/00086223.
7. Pinault M., Mayne-L'Hermite M., Reynaud C., Pichot V., Launois P. and Ballutaud D. (2005). Growth of multiwalled carbon nanotubes during the initial stages of aerosol-assisted CCVD. *Carbon* **43**, 2968–2976.
8. Rhoda R.N. and Vines R.F. (1969). *Bath and process for platinum and platinum alloys,* U.S. Patent 3,486,928.
9. Dale Minerals International. *X-ray Spacing.* Online at: http://www.webmineral.com/MySQL.
10. Kwon O-K., Kwon S-H., Park H-S. and Kang S.W. (2004). Plasma-enhanced atomic layer deposition of ruthenium thin films. *Electrochem. Solid State Lett.* **7**, C46–C48.
11. Tsou Y-M., Cao L. and de Castro E. (2004). Novel high performance platinum and alloy catalysts for PEMFC & DMFC. *Prepr. Pap.-Am. Chem. Soc., Div. Fuel Chem.* **49**, 679–680.
12. Guo J.W., Zhao T.S., Prabhuram J., Chen R. and Wong C.W. (2005). Preparation and characterisation of a PtRu/C nanocatalyst for direct methanol fuel cells. *Electrochim. Acta* **51**, 754–763.
13. Johnson Matthey™. *HiSPEC®* Catalyst Datasheet. Online at: http://www.johnsonmattheyfuelcells.com/HiSPEC_Datasheet.pdf.
14. Cabot™ Corporation. Online at: http://w1.cabot-corp.com/index.jsp
15. Prabhuram J., Zhao T.S., Wong C.W. and Guo J.W. (2004). Synthesis and physical/electrochemical characterisation of Pt/C nanocatalyst for polymer electrolyte fuel cells. *J. Power Sources* **134**, 1–6.
16. Jordan L.R., Shukla A.K., Behrsing J., Avery N.R., Muddle B.C. and Forsyth M. (2000). Effect of diffusion-layer morphology on the performance of polymer electrolyte fuel cells operating at atmospheric pressure. *J. Appl. Electrochem.* **30**, 641.
17. Long J.W., Stroud R.M., Swider-Lyons K.E. and Rolison D.R. (2000). How to make electrocatalysts more active for direct methanol oxidation – avoid PtRu bimetallic alloys! *J. Phys. Chem. B* **104**, 9772.
18. Steigerwalt E.S., Deluga G.A., Cliffel D.E. and Lukehart C.M. (2001). A Pt-Ru / graphitic carbon nanofiber nanocomposite exhibiting high relative performance as a direct-methanol fuel cell anode catalyst. *J. Phys. Chem. B* **105,** 8097–8101.
19. Jarvi T.D. and Stuve E.M. (1998). Fundamental aspects of vacuum and electrocatalytic reactions of methanol and formic acid on platinum surfaces. In *Electrocatalysis,* eds J. Lipkowski and P.N. Ross Jr., pp. 75–153. Wiley-VCH, New York.